

# Nonlinear resonance jump in turbine governor positioning system

Krunoslav Horvat, *student, IEEE*, Ognjen Kuljača, *student, IEEE*, and Ljubomir Kuljača

**Abstract**—The paper deals with analysis of turbine governor positioning system of hydropower plant regarding nonlinear resonance jump. The meaning of the term "resonance jump" is explained in the introduction. Then the description of the plant is given. Two methods of analyzing system with the respect to resonance jumps are described: the simulation method and the analytical method. When using the simulation method, the analysis of the variations of important parameters is performed. At the end, the confirmation of the results of simulation is given by the analytical method.

**Index Terms**—Electro-hydraulic system, hydropower plant, nonlinear resonance jump, nonlinear system

## I. INTRODUCTION

The term "resonance jump" is used in the case of a sudden jump of amplitude and/or frequency and/or phase of a periodic output signal of a nonlinear system. Resonance jump can occur in nonlinear systems and is often not desirable state in the system. Resonance jump cannot occur if excitation is such that the response of the system is transient and cannot be defined by solving nonlinear differential equations. It is also not recommended to use the experimental tests on the plant during operation in order to resolve if the system can have tendency to the occurrence of this phenomenon. For that purpose the best way is to use analytical and simulation methods.

## II. DESCRIPTION OF THE PLANT

The main parts of the analyzed plant (water turbine governor positioning system) are electro-hydraulic proportional valve and hydraulic servomotor. A position sensor is built in within the hydraulic servomotor. In the real system analyzed here the position controller was implemented using PLC (Programmable Logical Controller). Apart from the saturation inherent in hydraulic servomotor, the controller is also designed with the output saturation in order to insure that the maximal permitted velocity of the piston of the hydraulic servomotor will not be reached.

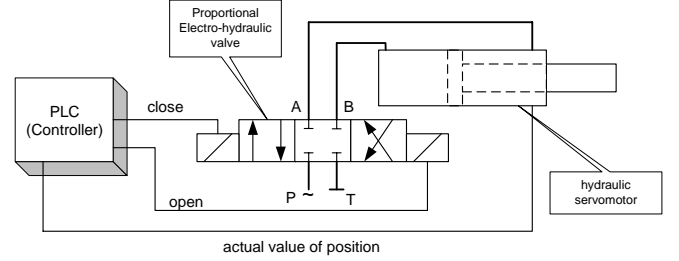


Fig. 1. Block diagram of the plant

## III. SIMULATION

### A. Simulation scheme

The scheme used for the simulation analysis is given in Fig. 2.

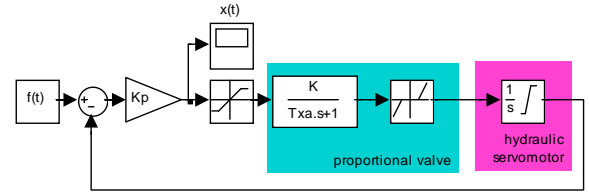


Fig. 2. Simulation scheme of the system

where:

$$f(t) = F_v \sin(\omega_v t) + F_{v0}; \quad F_{v0} = F_v \quad (1)$$

$$x(t) = X_m \sin(\omega_v t + \varphi_x) \quad (2)$$

Simulation analysis is preformed using Matlab with Simulink. The input excitation signal  $f(t)$  is generated using the Matlab script file that calls the Simulink model shown in Fig. 2.. It is actually a modified chirp signal, the frequency of which is changed every 100 seconds with step of 0.01 Hz. Signal  $x(t)$  is input of the nonlinear part of the system. Integrator that represents hydraulic servomotor has upper windup limit at 0.245 m and lower windup limit at 0 m.

K. Horvat is with Brodarski institute, Ave. V. Holjeveca 20, 10020 Zagreb, Croatia, e-mail: kruno@hrbi.hr

O. Kuljača is with Automation & Robotics Research Institute, The University of Texas at Arlington, 7300 J. Newell Blvd. South, TX 76118, USA, e-mail: okuljaca@arri.uta.edu

Lj. Kuljača is with Faculty of Electrical Engineering and Computing, The University of Zagreb, Unska 3, 10000 Zagreb, Croatia, e-mail: ljubomir.kuljaca@fer.hr

### B. Resonance jump for real parameters of system

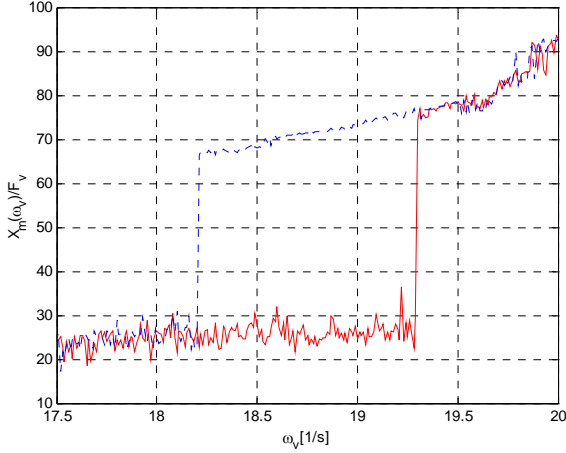


Fig. 3. Resonance jump generated with the real parameters of the system

The simulation with the real parameters of the system is shown in Fig. 3. Fig. 3 is the referent figure for all the other simulation figures. There are two curves in each simulation figure. The curve with the solid line represents the response on rising frequency, while the curve with the dashed line represent the response on falling frequency.

The real values of the parameters were:

TABLE I  
REAL VALUES OF PARAMETERS

parameter	value
upper and lower saturation limit	$\pm 0.3$ [p.u.]
start and end of dead zone	$\pm 0.06$ [p.u.]
upper windup of hydraulic servomotor	0.245 [m]
lower windup of hydraulic servomotor	0 [m]
K – gain of the electro-hydraulic valve	200
K <sub>p</sub> – gain of proportional controller	100
T <sub>xa</sub> -Time constant of the electro-hydraulic valve	0.8 [s]
F <sub>v</sub> – magnitude of excitation	0.1225
offset of excitation	0.1225

### C. Influence of saturation on resonance jump

In order to analyze the system on variation of saturation, the upper and lower saturation limits have changed into  $\pm 0.25$  p.u. The results are shown in Fig. 4. The case, where the saturation limits were changed into  $\pm 0.35$  p.u., is shown in Fig. 5.

From Figs 3 – 5, one can see, by comparison, that the resonance jumps exist in each case. The system exhibits the similar behavior in all three cases. However, the change of the saturation limits changes the frequencies at which the resonance jumps occur. For the smaller saturation limits the frequencies at which the resonance jump occurs are lower (compare Fig. 3 and Fig. 4). For the bigger saturation limits that frequencies are higher. The differences between the case are up to 2 Hz.

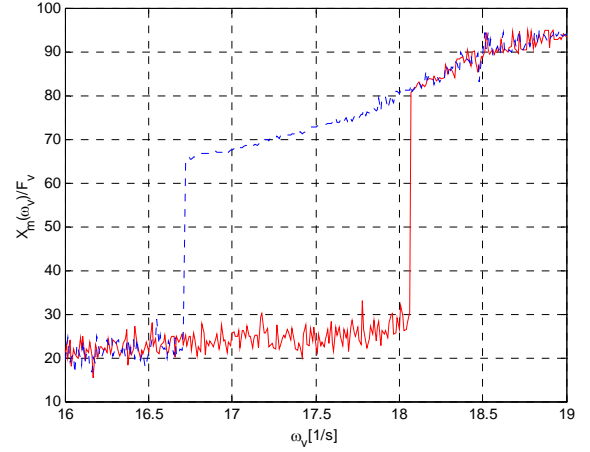


Fig. 4. Resonance jump with smaller saturation value than with the real parameters of the system

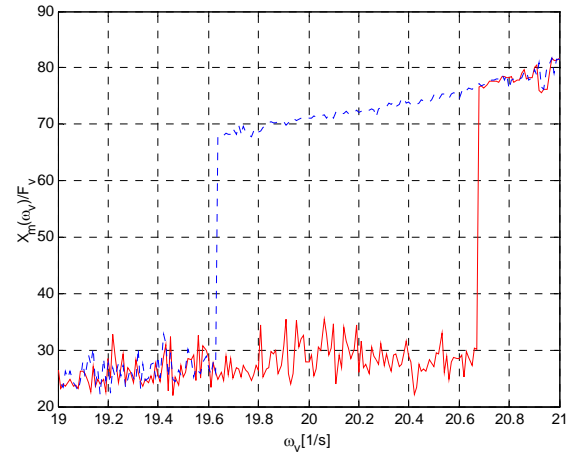


Fig. 5. Resonance jump with greater saturation value than with the real parameters of the system

### D. Influence of dead zone on resonance jump

The system was also analyzed on change of the dead zone with the respect to nonlinear resonance jump. The simulation results for the system without dead zone (all the other parameters were left as in Table 1.) are shown in Fig. 6 and the results for the case with augmented dead zone are shown in Fig. 7. The start and the end of dead zone have been from  $\pm 0.06$  p.u. changed to  $\pm 0.12$  p.u. The variations are 100% at every side of dead zone.

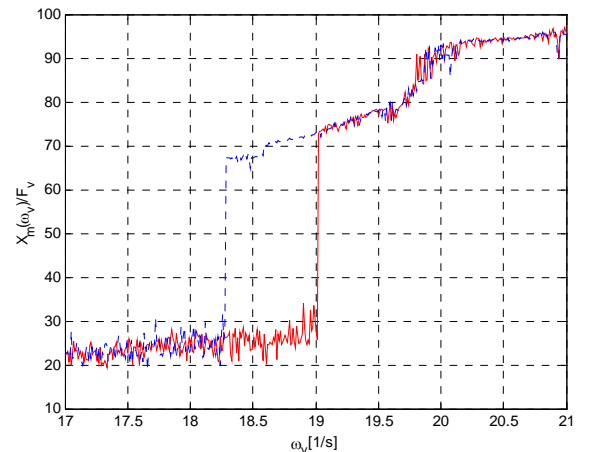


Fig. 6. Resonance jump without dead zone

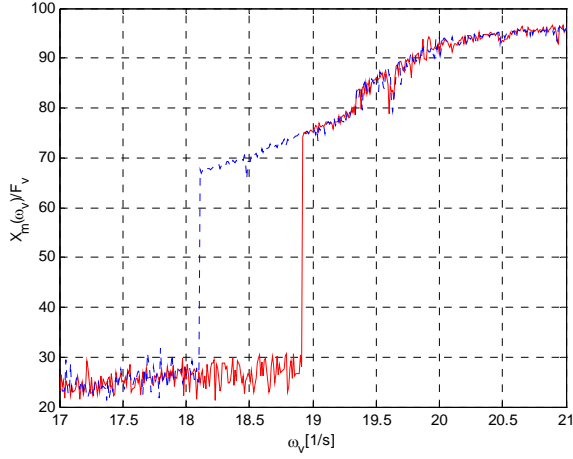


Fig. 7. Resonance jump with the greater value for dead zone than with the real parameters of the system

Comparison of the simulation results from Fig. 3, Fig. 6 and Fig. 7 shows that change in the dead zone limits does not affect the occurrence of the nonlinear jump in significant way. All the frequencies where the resonance jump occurred are almost the same (Figs 3, 6 and 7).

#### E. Influence of gain K of the electro-hydraulic valve on resonance jump

In order to analyze the influence of variation of the gain K of the electro-hydraulic valve, the value of the gain K was changed into 170. The results are shown in Fig. 8. Another case, with the value of the gain K equal to 230, is shown in Fig. 9.

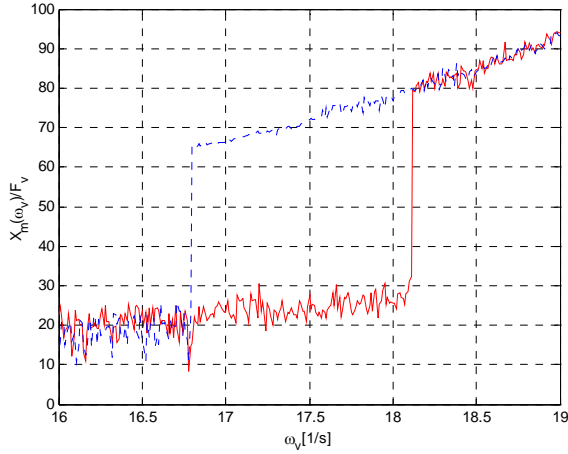


Fig. 8. Resonance jump with smaller value for gain K than with the real parameters of the system

Again, comparing the results in Figs 3, 8 and 9 one can note the differences. For the smaller K resonance jump occurs at the lower frequencies, for the bigger K at the higher frequencies. The difference between the cases is almost up to 2 Hz.

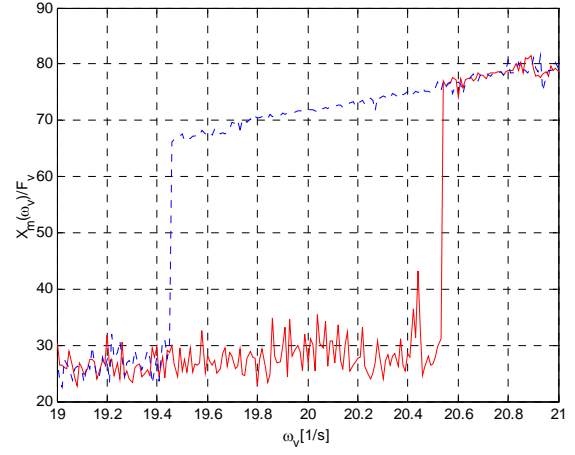


Fig. 9. Resonance jump with greater value for gain K than with the real parameters of the system

#### F. Influence of time constant Txa of the electro-hydraulic valve on resonance jump

To analyze the system on variation of the time constant Txa of the electro-hydraulic valve, the value of the time constant has been changed into 0.75. The results for that case are shown in Fig. 10. The results for the case with the value of time constant Txa equal to 0.9, are shown in Fig. 11.

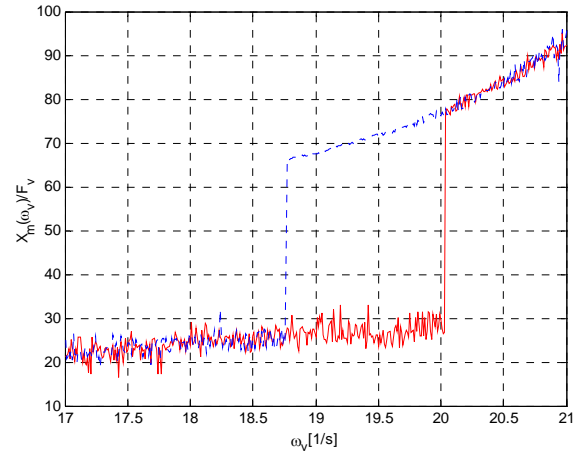


Fig. 10. Resonance jump with smaller value of Txa than with the real parameters of the system

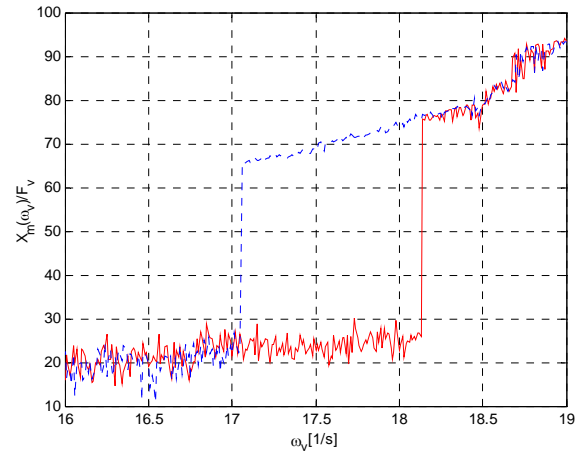


Fig. 11. Resonance jump with the greater value of Txa than with the real parameters of the system

Again, comparison of the simulation results from Figs. 3, 10 and 11 shows that the frequencies where resonance jump occurs are changed. The frequencies are lower for the greater value of. Txa

#### G. Resonance jump for real parameters of system and with symmetric excitation

For the purpose of comparison of the simulation approach and analytical approach the simulation with symmetric excitation has been performed. This case is shown in Fig. 12.

Here, the excitation signal has the following form:

$$f(t) = F_v \sin(\omega_v t) \quad (3)$$

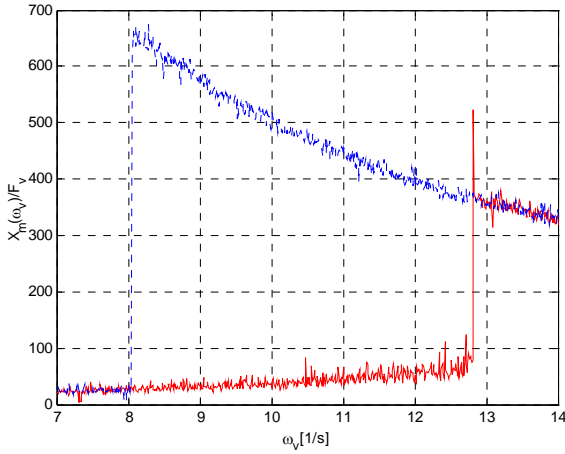


Fig. 12. Resonance jump for the real parameters of system and with symmetric excitation

One can note the sharp difference in the frequencies at which resonance jump occurs when this case is compared with the previous simulation results. Since we are dealing with the system that contains saturation, the big influence of the amplitude of the reference signal is expected.

#### H. Conclusion on simulation method

The simulation results given here lead to the following conclusion. The variations of saturation, gain K of the electro-hydraulic valve and the time constant Txa of the electro-hydraulic valve have big influence on resonance jump. Opposite to them, the variations of parameters of dead zone have very small influence on resonance jump and can be eliminated from further analysis. Of course, the elimination of dead zone is not always allowed. It is allowed only if the dead zone has very small influence on results of analysis. That can be always shown by the simulation. Thus, the simulation analysis is always a good starting point for the use of the analytical method.

### IV. ANALYTICAL METHOD

The resonance jump can be observed through analysis of frequency characteristics of nonlinear system.

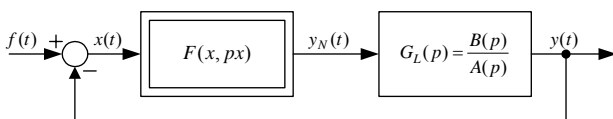


Fig. 13. Block diagram of a forced system

The quantities from Fig. 13 are:

$f(t) = F_v \sin(\omega_v t)$  - harmonic input to the system

$x(t) = X_m \sin(\omega_v t + \varphi_x)$  - input to the nonlinear part of the system

$F(x, px)$  - nonlinear part of the system

$G_L(p) = \frac{B(p)}{A(p)}$  - linear part of the system

The most suitable method to determine resonance jump of nonlinear system is the describing function method. The process of determining nonlinear resonance jump is based on equation (4)[1]:

$$X_m \frac{A(j\omega_v) + B(j\omega_v)[P(X_m, \omega_v) + jQ(X_m, \omega_v)]}{A(j\omega_v)} = F_v e^{-j\varphi_x} \quad (4)$$

which is for this purpose rewritten as:

$$X_m [1 + G_L(j\omega_v)G_N(X_m, \omega_v)] = F_v e^{-j\varphi_x} \quad (5)$$

where  $G_L(j\omega_v) = B(j\omega_v) / A(j\omega_v)$  is the linear part of the system,  $P(X_m, \omega_v)$  is the real part of the describing function of nonlinear part of the system,  $Q(X_m, \omega_v)$  is imaginary part of the describing function of the nonlinear part of the system,  $F_v e^{-j\varphi}$  is harmonic input to the system (excitation) and  $X_m$  represents the magnitude of the input of the nonlinear part of the system.

The area in which resonance jumps of magnitude  $X_m(\omega_v)$  can occur is determined by the envelope of family of circles.

To determine the frequency area where the occurrence of resonance jump is possible, the parametric equation (6) [1] of the envelope have to be determined by:

$$U(\omega_v) = - \frac{P \left( 2 \frac{dP}{dX_m} + X_m \frac{d^2 P}{dX_m^2} \right) + \frac{dP}{dX_m} \left( P + X_m \frac{dP}{dX_m} \right)}{P^2 \left( 2 \frac{dP}{dX_m} + X_m \frac{d^2 P}{dX_m^2} \right) + \frac{dP}{dX_m} \left( P + X_m \frac{dP}{dX_m} \right)^2} \quad (6)$$

$$V(\omega_v) = \pm \frac{-X_m \frac{dP}{dX_m} \sqrt{\frac{dP}{dX_m} \left( 2 \frac{dP}{dX_m} + X_m \frac{d^2 P}{dX_m^2} \right)}}{P^2 \left( 2 \frac{dP}{dX_m} + X_m \frac{d^2 P}{dX_m^2} \right) + \frac{dP}{dX_m} \left( P + X_m \frac{dP}{dX_m} \right)^2}$$

Consider our system:

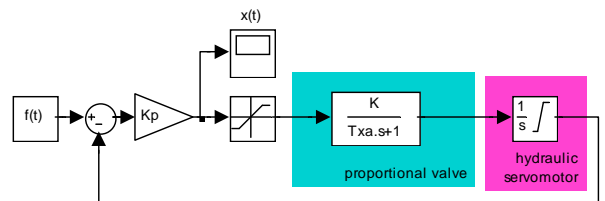


Fig. 14. Block structure of plant for the analytical method

Linear part of the system is:

$$G_L(s) = \frac{K}{s(T_{xa} + 1)} \quad (7)$$

or:

$$\begin{aligned} G_L(j\omega_v) &= \frac{K}{j\omega_v(j\omega_v T_{xa} + 1)} \\ &= -\frac{KT_{xa}}{1 + \omega_v^2 T_{xa}^2} - j \frac{K}{\omega_v(1 + \omega_v^2 T_{xa}^2)} \\ &= U(\omega_v) + jV(\omega_v) \end{aligned} \quad (8)$$

The describing function of nonlinear part of the system is:

$$G(X_m, b) = P(X_m, b) = \frac{2}{\pi} \left( \arcsin \frac{b}{X_m} + \frac{b}{X_m} \sqrt{1 - \frac{b^2}{X_m^2}} \right) \quad (9)$$

$$; X_m \geq b$$

where b is upper and lower limit saturation.

From (6) it follows:

$$\frac{dP}{dX_m} = \frac{4b}{\pi} \frac{b^2 - X_m^2}{X_m^3 \sqrt{X_m^2 - b^2}} \quad (10)$$

$$\frac{d^2 P}{dX_m^2} = \frac{4b}{\pi} \frac{2X_m^2 - 3b^2}{X_m^4 \sqrt{X_m^2 - b^2}} \quad (11)$$

From (8), (9) and (10), for  $b = 0.3$  we obtain:

$$P(X_m) = \frac{2}{\pi} \left( \arcsin \frac{0.3}{X_m} + \frac{0.3}{X_m} \sqrt{1 - \frac{0.3^2}{X_m^2}} \right); \quad (12)$$

$$X_m \geq 0.3$$

$$\frac{dP}{dX_m} = \frac{1.2}{\pi} \frac{0.09 - X_m^2}{X_m^3 \sqrt{X_m^2 - 0.09}} \quad (13)$$

$$\frac{d^2 P}{dX_m^2} = \frac{1.2}{\pi} \frac{2X_m^2 - 0.27}{X_m^4 \sqrt{X_m^2 - 0.09}} \quad (14)$$

From (7) and (8) for  $K = 200$  and  $T_{xa} = 0.8$  we obtain:

$$G_L(s) = \frac{200}{s(0.8s + 1)} \quad (15)$$

$$U = -\frac{160}{1 + 0.8^2 \omega_v^2}; \quad V = -\frac{200}{\omega_v(1 + 0.8^2 \omega_v^2)} \quad (16)$$

$$V^2 = -\frac{U^3}{U + KT}; \quad U > -160$$

By substituting obtained relations into (6), the crossing points of the parametric equation of the envelope and the equation of the linear part are determined. The area of resonance jump is defined by frequency interval  $(\omega_{v1}, \omega_{v2})$ .

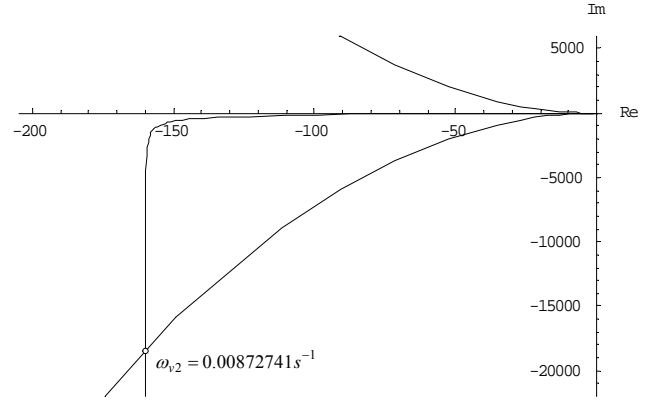


Fig. 15. Frequency characteristic of linear part of the system  $G_L(j\omega_v)$  and envelope of nonlinear part of the system

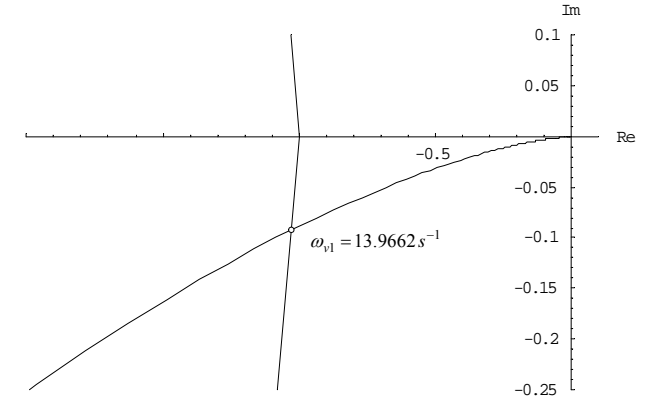


Fig. 16. Frequency characteristic of linear part of the system  $G_L(j\omega_v)$  and envelope of nonlinear part of the system - Detail

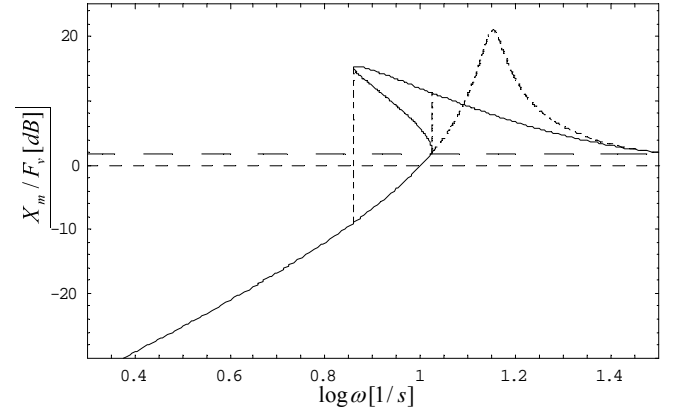


Fig. 17. The frequency characteristic  $X_m(\omega_v)$  determined analytically (dashed line is linear system frequency response)

## V. CONCLUSION

Since the nonlinear resonance jump phenomenon can degrade dynamics of the nonlinear system. Its analysis is recommended. In most cases the experimental analysis on the real system is not possible. For the complex systems analytical method is difficult or even impossible. So, the only way to perform the analysis of complex nonlinear systems is often simulation approach. The approaches presented in this paper can significantly improve design of nonlinear control systems. The results of the analysis can point out which operating regimes should be avoided so that the system does not operate in the area where the nonlinear resonance jump can occur. It is also possible to determine the elements to be added in control loop/circuit in order to

modify the phase of the whole system in such way that the resonance jumps are avoided.

#### REFERENCES

- [1] Z. Vukić, Lj. Kuljača, D. Đonlagić, S. Tešnjak, *Nonlinear Control Systems*, Dekker, ISBN:0-8247-4112-9, 2003
- [2] O. Kuljaca, Lj. Kuljaca, Z. Vukic, S. Bruno, *Fuzzy controller for elimination of the nonlinear resonance phenomenon*, Proceedings of 10<sup>th</sup> Mediterranean Conference on Control and Automation – MED2002, Lisbon, Portugal, July 9-12, 2002.
- [3] B. Strah, *Hydroturbine Control with Fault Detection in the Positioning of Gate Regulating Ring* - Master's Thesis, Faculty of Electrical Engineering and Computer Science, University of Zagreb, 2000 (in Croatian)
- [4] A. Isidori, *Nonlinear Control Systems*, Springer-Ferlag, Berlin, 1995.
- [5] Lj. Kuljača, Z. Vukić, D. Đonlagić, S. Tešnjak, *Nonlinear Systems of Automatic Control*, University of Maribor, Maribor 1998. (in Slovenian)
- [6] Netushil at al. *Theory of Automatic Control*, Mir, Moscow 1978
- [7] E. N. Rosenwaser, *Oscillations of Nonlinear Control Systems*, Mashinostroenie, Moscow, 1989, (in Russian)